

Research Article

Vortex Structures in Optical Fibers Under the Influence of Third-Order Dispersion and Self-Steepening Effect

Aneliya Dakova-Mollova^{1,2*}, Nikol Gocheva², Valeri Slavchev^{1,3}, Zara Kasapeteva^{1,4}, Diana Dakova², Anjan Biswas^{5,6,7}, Lubomir Kovachev¹

¹Institute of Electronics, Bulgarian Academy of Sciences, 72 Tzarigradsko shossee, 1784, Sofia, Bulgaria

²Physics and Technology Faculty, University of Plovdiv "Paisii Hilendarski", 24 Tsar Asen Str., 4000, Plovdiv, Bulgaria

³Faculty of Pharmacy, Medical University-Plovdiv, 15 Vasil Aprilov Bul., 4002, Plovdiv, Bulgaria

⁴Faculty of Mechanical Engineering, Technical University Sofia-Plovdiv Branch, 25 Tzanko Diustabanov Str., 4000, Plovdiv, Bulgaria

⁵Department of Mathematics and Physics, Grambling State University, 403 Main Street, Grambling, LA-71245, USA

⁶Department of Applied Sciences, Cross-Border Faculty of Humanities, Economics and Engineering, Dunarea de Jos University of Galati, 111 Domneasca Street, Galati, 800201, Romania

⁷Department of Mathematics and Applied Mathematics, Sefako Makgatho Health Sciences University, Medunsa, 0204, Pretoria, South Africa

E-mail: anelia.dakova@gmail.com

Received: 30 September 2024; Revised: 16 January 2025; Accepted: 22 January 2025

Abstract: The present paper for the first time it is investigated the generation and formation of amplitude-type vortices, propagating in single-mode optical fibers with step-index profile under the influences of third-order dispersion and self-steepening effect or so called dispersion of nonlinearity of the medium. The main model includes the vector nonlinear amplitude equation, from which a system of two scalar partial differential equations is derived. They describe the evolution of the x and y components of the vector amplitude function \vec{A} of an optical pulse under the influences of these higher order nonlinear and dispersive phenomena. New exact analytical solutions of the resulting system of equations were obtained in the form of optical vortices. They have amplitude type singularity and they are observed as ring structures in the components of the laser pulses. Numerical simulations of the found solutions are performed. It is shown that the vortex parameter m is related to the number of these ring structures. Significant depolarization of the vector electric field in the spot of the laser radiation is registered.

Keywords: nonlinear amplitude equation, optical vortices, third-order dispersion, self-steepening effect

1. Introduction

Vortex structures are optical beams or pulses that possess a singularity in the amplitude or phase. Normally, they are observed out of the laser resonator. Vortices are obtained by optical masks and computer-synthesized holograms [1-6]. Such structures in light beams can be described by the well-known 2D Leontovich equation in scalar form [7-8]. Laser vortex structures are characterized by spiral phase allocation or angular dependence of the electric field.

In the last few decades, the author has made remarkable progress in researching the formation and propagation of different kinds of laser vortices [9-11]. The peculiarities of their evolution open up new possibilities for their potential

Copyright ©2025 Aneliya Dakova-Mollova, et al.

DOI:

This is an open-access article distributed under a CC BY license
(Creative Commons Attribution 4.0 International License)
<https://creativecommons.org/licenses/by/4.0/>

application in several modern technologies, such as quantum information transfer, data encryption, high-resolution laser microscopy, optical tweezers, optical vortex trapping, and many others [12-17]. Their evolution in various waveguides is practically studied in [18-21]. Optical vortices with ring structures in the components of the electric field were found in [22]. In recent years, the study of laser vortices, characterized by amplitude type singularities, has been quite relevant. Such kinds of vortices were newly reported in [23]. It is characteristic of them that they are observed as concentric circles in the laser pulse components. These light rings are due to the modulations in the amplitude. Their dynamics in single-mode fibers with step-index profiles were studied analytically for the first time in the frames of the vector nonlinear amplitude equation (NAE) by authors in [24]. This equation was reduced to a system of two partial differential equations, describing the components of the vector amplitude function. Here, it is important to mention that these laser circles can be seen only in the amplitude's components. In the spot of the optical pulse, the light rings are not noticeable, because the maxima of one component coincide with the minima of the other. In this way, compensation in their rotation is realized. The presence of amplitude type vortices is registered by the diagram, visualizing the orientation of the vector electric field of the pulses.

On the other hand, the advances in the investigations of ultra-short high-intensity laser pulses and their increasing use in modern photonic technologies necessitate the study of the effects that accompany the evolution of these wave packages. It is well-known that phase-modulated optical pulses or those in the femtosecond and attosecond regions are characterized by a broad-band spectrum for which $\Delta\lambda \approx \lambda_0$ (λ_0 is the carrier wavelength, $\Delta\lambda$ is the initial bandwidth of the pulse). For such optical pulses, it is necessary to take into account higher order nonlinear and dispersive effects such as third-order dispersion (TOD) and self-steepening effect or so called dispersion of nonlinearity (DN). In the femtosecond region, even when the group velocity dispersion (GVD) is nonzero, TOD needs to be considered. The influences of GVD and TOD on the optical pulse result in asymmetry in its shape. Oscillatory structures can be seen on one of its edges depending on the sign of TOD [25]. Near the zero-dispersion wavelength, these oscillations become deeper and the intensity drops to zero. The propagation of ultra-short laser pulses in optical fibers may be accompanied by the effect of dispersion of nonlinearity. This is a higher-order nonlinear phenomenon that arises from the dependence of the pulse's group velocity on its intensity. That leads to temporal and spectral changes in light pulses and can generate so called optical shock waves in waveguides with low losses [26-29]. These two effects can seriously affect the evolution of ultra-short laser pulses in single-mode optical fibers. Similar effects have been studied analytically in the case of the formation and evolution of optical solitons in various media [30-35]. This convinced us that it is necessary to take into account higher orders of dispersion and nonlinearity in the case of laser vortex structures propagating in single-mode optical fibers.

During our analytical investigations, we chose to work with the more general vector NAE, which has a number of advantages over the standard nonlinear Schrödinger equation (NSE) [36]. It differs from NSE with two terms that depend on the initial pulse duration (T_0). As a result, NAE can be used for characterizing the evolution of long, as well as ultra-short laser pulses. In the present case, NAE includes additional parameters responsible for TOD and DN.

The main idea of the current paper is to find new exact analytical solutions for the vector NAE, presenting the peculiarities in the dynamics of vortex structures in optical fibers with step-index profiles under the influences of third-order dispersion and self-steepening effect. The found solutions are characterized by amplitude-type singularity. Vortices are observed in the form of ring structures in the components of the laser pulses. It is shown that the vortex parameter m is related to the number of these laser circles. Parameters connected with nonlinearity are included in the derived expression for the vortex parameter m . Therefore, they influence the number of ring structures. It turns out that the second and third-order dispersion changes the phase of the components of the optical pulse. It does not directly affect the formation of the optical vortex. Significant depolarization of the vector electric field in the spot of the laser radiation is registered in the presented figures.

The rest of this paper is structured as such. Section 2 presents the main mathematical model on which the paper is based. The analytical solution of the system of nonlinear amplitude equations is presented in detail and the corresponding solutions in the form of optical vortices are derived. In Section 3, several figures are shown, made through numerical simulations based on the obtained analytical solutions. Finally, a few concluding words are noted in Section 4.

2. Main equation

The evolution of laser vortex in single-mode fiber with step-index profile and anomalous dispersion, under the influences of TOD and DN is given by the following equation in vector form [25, 36]:

$$i\frac{\partial \vec{A}}{\partial \xi} - \frac{\beta}{2\alpha} \frac{\partial^2 \vec{A}}{\partial \tau^2} + \frac{1}{2\alpha} \left(\frac{\partial^2 \vec{A}}{\partial \xi^2} - 2 \frac{\partial^2 \vec{A}}{\partial \xi \partial \tau} \right) - \frac{i\sigma}{2\alpha} \frac{\partial^3 \vec{A}}{\partial \tau^3} + \frac{1}{2\alpha} \Delta_{\perp} \vec{A} + \gamma |\vec{A}|^2 \vec{A} + is\gamma \frac{\partial}{\partial \tau} (|\vec{A}|^2 \vec{A}) = 0, \quad (1)$$

where

$$\begin{aligned} \xi &= \frac{z'}{z_0}, \quad \tau = \frac{t - \frac{z'}{v_{gr}}}{T_0}, \quad \Delta_{\perp} = \frac{\partial^2}{\partial x^2} + \frac{\partial^2}{\partial y^2}, \quad x = \frac{x'}{r_0}, \quad y = \frac{y'}{r_0}, \quad A = \frac{A}{A_0}, \\ \alpha &= k_0 z_0, \quad \gamma = k_0^2 r_{\perp}^2 n_2 |A_0|^2, \quad \beta = k_0 v_{gr}^2 |k''|, \quad \sigma = \frac{2}{\omega_0 T_0} + \frac{1}{\chi^{(3)} T_0} \frac{\partial \chi^{(3)}}{\partial \omega} = \frac{\beta}{\alpha} \left(1 + \frac{k_0 c k'''}{n_0 k''} \right). \end{aligned} \quad (2)$$

The equation (1) \vec{A} is the vector amplitude function and Δ_{\perp} is the transverse Laplace operator. The number of oscillations of the electric field at level l/e of the amplitude function's maximum is presented by the constant α , β is connected with the second-order dispersion of the medium, γ is related to the Kerr-type nonlinearity of the waveguide, σ characterizes third-order dispersion and s is the self-steepening parameter. In the expressions above A_0 and T_0 stand for the initial amplitude function and initial time duration of the pulse, k_0 is the wave number, k'' and k''' are second and third derivatives of the wave number, z_0 and r_{\perp} are respectively the initial longitudinal and transverse sizes of the laser pulse, v_{gr} is the group velocity, n_0 and n_2 present the linear and nonlinear refractive index of the waveguide, $\chi^{(3)}$ is the dielectric susceptibility of the medium, ω_0 is the carrier frequency, c is constant, t is time and x' , y' , z' are Cartesian coordinates. The vector amplitude function of the laser pulse is of the kind $\vec{A} = (A_x(x, y, \xi, \tau), A_y(x, y, \xi, \tau), 0)$. Having in mind the geometry of the optical fiber, we can go from local time coordinate system to cylindrical coordinates:

$$x = r \cos \theta, \quad y = r \sin \theta,$$

$$r = \sqrt{x^2 + y^2}, \quad \theta = \arctan \left(\frac{y}{x} \right). \quad (3)$$

After some calculations, from the basic equation (1) we derive the following system of scalar partial differential equations, describing the components A_x and A_y of the vector field. The equations are presented in polar coordinates. They give the features in the dynamics of ultra-short laser pulses in single-mode optical fibers. The system of equations is in the form:

$$\begin{aligned} i\frac{\partial A_x}{\partial \xi} - \frac{\beta}{2\alpha} \frac{\partial^2 A_x}{\partial \tau^2} + \frac{1}{2\alpha} \left(\frac{\partial^2 A_x}{\partial \xi^2} - 2 \frac{\partial^2 A_x}{\partial \xi \partial \tau} \right) + \frac{1}{2\alpha} \left[\frac{1}{r} \frac{\partial A_x}{\partial r} + \frac{\partial^2 A_x}{\partial r^2} + \frac{1}{r^2} \frac{\partial^2 A_x}{\partial \theta^2} \right] \\ - \frac{i\sigma}{2\alpha} \frac{\partial^3 A_x}{\partial \tau^3} + \gamma |A_x^2 + A_y^2| A_x + is\gamma \frac{\partial}{\partial \tau} (|A_x^2 + A_y^2| A_x) = 0, \end{aligned} \quad (4)$$

$$i \frac{\partial A_y}{\partial \xi} - \frac{\beta}{2\alpha} \frac{\partial^2 A_y}{\partial \tau^2} + \frac{1}{2\alpha} \left(\frac{\partial^2 A_y}{\partial \xi^2} - 2 \frac{\partial^2 A_y}{\partial \xi \partial \tau} \right) + \frac{1}{2\alpha} \left[\frac{1}{r} \frac{\partial A_y}{\partial r} + \frac{\partial^2 A_y}{\partial r^2} + \frac{1}{r^2} \frac{\partial^2 A_y}{\partial \theta^2} \right] - \frac{i\sigma}{2\alpha} \frac{\partial^3 A_y}{\partial \tau^3} + \gamma |A_x^2 + A_y^2| A_y + is\gamma \frac{\partial}{\partial \tau} (|A_x^2 + A_y^2| A_y) = 0. \quad (5)$$

As a next step in our theoretical model, we will use the method of separation of variables to transform the components of the vector amplitude function A_x and A_y . We are making the assumption that the system of equations (4) and (5) supports solutions for the components A_x and A_y of the kind:

$$A_x(r, \theta, \xi, \tau) = T_x P_x(r, \theta) \exp[i\Psi_x(\xi, \tau)],$$

$$A_y(r, \theta, \xi, \tau) = T_y P_y(r, \theta) \exp[i\Psi_y(\xi, \tau)], \quad (6)$$

where $\Psi_x(\xi, \tau) = \Psi_y(\xi, \tau) = a\tau + b\xi$ is the generalized phase. In this expression a and b are constants. We find the derivatives of (6) and we substitute them in the system of equations (4) and (5). Thus, we obtain the following two partial differential equations of third order and third degree for the four unknown functions (P_x , P_y , T_x and T_y) of three independent variables τ , r and θ :

$$-2\alpha b P_x T_x + \beta (T_x'' + 2iaT_x' - a^2 T_x) P_x - (b^2 T_x + 2ibT_x' - 2abT_x) P_x - i\sigma (T_x''' + 3iaT_x'' - 3a^2 T_x' - ia^3 T_x) P_x + \quad (7)$$

$$T_x \left(\frac{1}{r} \frac{\partial P_x}{\partial r} + \frac{\partial^2 P_x}{\partial r^2} + \frac{1}{r^2} \frac{\partial^2 P_x}{\partial \theta^2} \right) + 2\alpha\gamma(1-as) |P_x^2 T_x^2 + P_y^2 T_y^2| P_x T_x = 0,$$

$$-2\alpha b P_y T_y + \beta (T_y'' + 2iaT_y' - a^2 T_y) P_y - (b^2 T_y + 2ibT_y' - 2abT_y) P_y - i\sigma (T_y''' + 3iaT_y'' - 3a^2 T_y' - ia^3 T_y) P_y + \quad (8)$$

$$T_y \left(\frac{1}{r} \frac{\partial P_y}{\partial r} + \frac{\partial^2 P_y}{\partial r^2} + \frac{1}{r^2} \frac{\partial^2 P_y}{\partial \theta^2} \right) + 2\alpha\gamma(1-as) |P_y^2 T_y^2 + P_x^2 T_x^2| P_y T_y = 0,$$

where T' and T'' are denoted the corresponding ordinary derivatives with respect to the variable τ . In a number of papers [37-39], it has been shown that in the one-dimensional scalar case for a medium with anomalous dispersion, equation (1) has a soliton solution $A = A(\xi, \tau) = T(\tau) \exp[i\psi(\xi, \tau)]$. We assume that both components of the laser pulse have the same dependencies. Therefore, in the case under consideration, the amplitude function for a fundamental soliton is of the kind:

$$T = T_x = T_y = \text{sech}(\tau) = \frac{1}{\text{ch}(\tau)}. \quad (9)$$

The energy of each of the components A_x and A_y of the amplitude function is given by the expressions [36]:

$$E_x = \int_{-\infty}^{+\infty} |A_x^2| d\tau = |P_x^2| \int_{-\infty}^{+\infty} T^2 d\tau, \quad (10)$$

$$E_y = \int_{-\infty}^{+\infty} |A_y^2| d\tau = |P_y^2| \int_{-\infty}^{+\infty} T^2 d\tau. \quad (11)$$

Considering formula (9), we obtain:

$$E_x = 2 |P_x^2|, \quad (12)$$

$$E_y = 2 |P_y^2|. \quad (13)$$

Therefore, the energies of the two components A_x and A_y are determined by the square of the modulus of the unknown functions P_x and P_y , respectively. This gives us reason to eliminate the variable τ in equations (7) and (8). For this purpose, we multiply the two equations by T and then we integrate them. Bearing in mind that, we find:

$$\int_{-\infty}^{+\infty} T^2 d\tau = 2, \quad (14)$$

$$\int_{-\infty}^{+\infty} T' T d\tau = 0, \quad (15)$$

$$\int_{-\infty}^{+\infty} T'' T d\tau = -\frac{2}{3}, \quad (16)$$

$$\int_{-\infty}^{+\infty} T''' T d\tau = 0, \quad (17)$$

$$\int_{-\infty}^{+\infty} T^4 d\tau = \frac{4}{3}. \quad (18)$$

After integration and short transformations, we obtain the following system of partial differential equations for the unknown functions P_x and P_y :

$$-\sigma a^3 - \sigma a - 2\alpha b + \beta a^2 - b^2 + 2ab - \frac{\beta}{3} + \frac{1}{P_x} \left(\frac{1}{r} \frac{\partial P_x}{\partial r} + \frac{\partial^2 P_x}{\partial r^2} + \frac{1}{r^2} \frac{\partial^2 P_x}{\partial \theta^2} \right) \quad (19)$$

$$+ \frac{4}{3} \alpha \gamma (1 - as) |P_x^2 + P_y^2| = 0,$$

$$\begin{aligned}
& -\sigma a^3 - \sigma a - 2\alpha b + \beta a^2 - b^2 + 2ab - \frac{\beta}{3} + \frac{1}{P_y} \left(\frac{1}{r} \frac{\partial P_y}{\partial r} + \frac{\partial^2 P_y}{\partial r^2} + \frac{1}{r^2} \frac{\partial^2 P_y}{\partial \theta^2} \right) \\
& + \frac{4}{3} \alpha \gamma (1 - as) |P_x^2 + P_y^2| = 0.
\end{aligned} \tag{20}$$

Our mathematical model requires us to assume that:

$$-\sigma a^3 - \sigma a - 2\alpha b + \beta a^2 - b^2 + 2ab - \frac{\beta}{3} = 0, \quad \frac{4}{3} \alpha \gamma (1 - as) = C = \text{const.} \tag{21}$$

After the assumptions made (21) and after a couple of transformations, the system of equations (19) and (20) can be presented as follows:

$$\frac{1}{r} \frac{\partial P_x}{\partial r} + \frac{\partial^2 P_x}{\partial r^2} + \frac{1}{r^2} \frac{\partial^2 P_x}{\partial \theta^2} + C |P_x^2 + P_y^2| P_x = 0, \tag{22}$$

$$\frac{1}{r} \frac{\partial P_y}{\partial r} + \frac{\partial^2 P_y}{\partial r^2} + \frac{1}{r^2} \frac{\partial^2 P_y}{\partial \theta^2} + C |P_x^2 + P_y^2| P_y = 0. \tag{23}$$

We search for a solution for that system in the form:

$$P_x = R_x(r) e^{in\theta}, \quad P_y = R_y(r) e^{in\theta}, \tag{24}$$

where $n = \text{const.}$

By using the substitutions (24) in equations (22) and (23) we obtain:

$$\frac{1}{r} \frac{\partial R_x}{\partial r} + \frac{\partial^2 R_x}{\partial r^2} - \frac{n^2}{r^2} \frac{\partial^2 R_x}{\partial \theta^2} + C |R_x^2 + R_y^2| R_x = 0, \tag{25}$$

$$\frac{1}{r} \frac{\partial R_y}{\partial r} + \frac{\partial^2 R_y}{\partial r^2} - \frac{n^2}{r^2} \frac{\partial^2 R_y}{\partial \theta^2} + C |R_x^2 + R_y^2| R_y = 0. \tag{26}$$

The resulting system contains two ordinary nonlinear differential equations, but this time of second order and third degree for the unknown functions R_x and R_y of one variable r . We notice that the nonlinear terms in both equations are the same, which means that the expressions can easily be linearized. For this purpose, we make assumptions so that when writing the new equations, the nonlinear terms are dropped:

$$R_x(r) = f(r) \cos(mr^q), \quad R_y(r) = f(r) \sin(mr^q), \tag{27}$$

where m and q are new constants about to be defined. By replacing the expressions (27) in the system of equations (25) and (26) and after few transformations, we obtain the following algebraic equations:

$$\cos(mr^q) \left(\frac{f'}{f} + f'' - fm^2q^2r^{2q-2} - \frac{n^2f}{r^2} + Cf^3 \right) \quad (28)$$

$$+ \sin(mr^q) (fmqr^{q-2} + 2f'mqr^{q-1} + fmq(q-1)r^{q-2}) = 0,$$

$$\sin(mr^q) \left(\frac{f'}{f} + f'' - fm^2q^2r^{2q-2} - \frac{n^2f}{r^2} + Cf^3 \right) \quad (29)$$

$$+ \cos(mr^q) (fmqr^{q-2} + 2f'mqr^{q-1} + fmq(q-1)r^{q-2}) = 0.$$

For the above equalities to be fulfilled, the expressions in front of the trigonometric functions must be equal to 0. Therefore, it is convenient to compile the following system:

$$\frac{f'}{f} + f'' - fm^2q^2r^{2q-2} - \frac{n^2f}{r^2} + Cf^3 = 0, \quad (30)$$

$$fmqr^{q-2} + 2f'mqr^{q-1} = 0. \quad (31)$$

From the second equation of the system above we determine:

$$f' = -\frac{q}{2} \frac{f}{r}. \quad (32)$$

The expression above is an equation with separable variables. After separating the variables and integrating them, we obtain the following solution:

$$f(r) = Nr^{-\frac{q}{2}}, \quad (33)$$

where N is an integration constant. We return to equation (30). By taking into account the expression (33) we obtain the following equation:

$$Nr^{-\frac{q}{2}-2} \left(\frac{q^2}{4} - m^2q^2r^{2q} - n^2 + CN^2r^{2-q} \right) = 0. \quad (34)$$

To satisfy the equality above, we assume that the expression in the brackets is zero:

$$\left(\frac{q^2}{4} - n^2 \right) + (CN^2r^{2-q} - m^2q^2r^{2q}) = 0. \quad (35)$$

We equate the powers of the variable r and thus, we find the value of the parameter q :

$$q = \frac{2}{3}. \quad (36)$$

Having in mind equation (36), from equation (35) we can find expressions for the parameters n and m . The first term in equation (35) is a constant that we equate to zero, and the second term is a function of r only. For equality (35) to be satisfied, we set the coefficient in front of r to be zero as well. Therefore:

$$m = N\sqrt{3\alpha\gamma(1-as)}, \quad (37)$$

$$n = \pm \frac{1}{3}. \quad (38)$$

After finding values for q , m , and n we return through all the assumptions and substitutions made so far. Thus, we defined the following exact analytical solutions for the components A_x and A_y of the vector amplitude function \vec{A} :

$$A_x = Nr^{-\frac{1}{3}} \cos\left(mr^{\frac{2}{3}}\right) e^{i(a\tau+b\xi+\frac{\theta}{3})}, \quad (39)$$

$$A_y = Nr^{-\frac{1}{3}} \sin\left(mr^{\frac{2}{3}}\right) e^{i(a\tau+b\xi+\frac{\theta}{3})}, \quad (40)$$

where

$$b_{1/2} = (a - \alpha) \left[1 \pm \sqrt{1 - \frac{a^2(\sigma a + \beta) + \sigma a + \frac{\beta}{3}}{(a - \alpha)^2}} \right]. \quad (41)$$

The exact analytical solutions (39) and (40) of the system of equations (4) and (5) for the components A_x and A_y of the vector amplitude function \vec{A} describe the formation of optical vortex structures in single-mode fibers with step-index profile under the influences of TOD and DN. The vortex parameter m is related to the number of rings observed in the components of the optical vortices. It has to be a real number. For this condition to be fulfilled it is necessary that $a < 1/s$. In the case of weak dispersion of nonlinearity $\left(\frac{\partial\chi^{(3)}}{\partial\omega} \approx 0\right)$, we can assume that the self-steepening parameter $s \approx 2/\alpha$. The obtained analytical expressions describe vortex structures with an amplitude type of singularity.

3. Numerical calculations

As a next step in our research, we will present numerical simulations, performed based on the obtained analytical solutions (39) and (40) of the vector NAE (1). It investigated a single-mode optical fiber with a step-index profile and a nonlinearity parameter $\gamma = 1$. Two cases for ultra-short pulses with $\alpha = 4$ are studied, when the vortex parameter is $m = 2$ and $m = 4$.

The present paper aims to show the existing dependencies between the number and type of ring structures in the intensity profiles of the components A_x and A_y of the vector amplitude function \vec{A} , the orientation of the vector electric field and the vortex parameter m .

Figure 1 shows the intensity profiles of the components A_x and A_y of optical pulse for vortex parameter $m = 2$ and number of oscillations under the pulse envelope $\alpha = 4$. The typical ring structures for this type of amplitude vortices are observed. Figure 2 gives the pulse's spot (total intensity) and the vector diagram of the optical vortex.

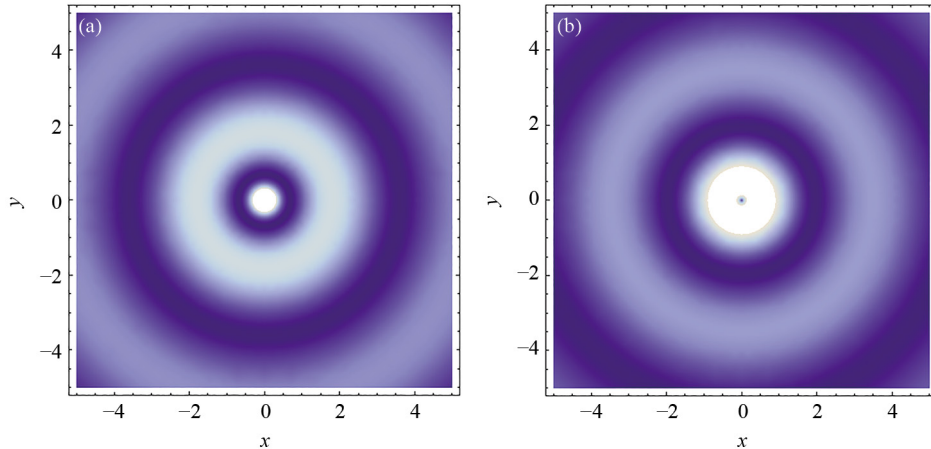


Figure 1. Optical ring structures in the intensity profiles of the components (a) A_x and (b) A_y of laser vortex with parameters $m = 2$ and $\alpha = 4$

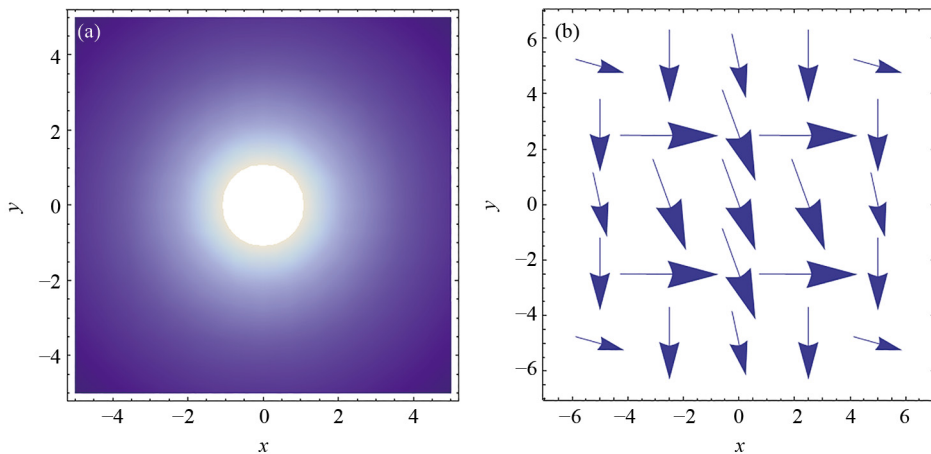


Figure 2. Graph of (a) the total intensity profile and (b) vector diagram of optical vortex with parameters $m = 2$ and $\alpha = 4$

Figure 3 presents the intensity profiles of the components A_x and A_y of the pulse for the value of the vortex parameter and $m = 4$ and the number of oscillations under the pulse envelope $\alpha = 4$. Concentric circles continue to be observed in the components of the vector amplitude \vec{A} of the vortex. The number of ring structures increases and their width decreases (Figure 3). Figure 4 shows the total intensity of the laser pulse and the orientation of its vector electric field.

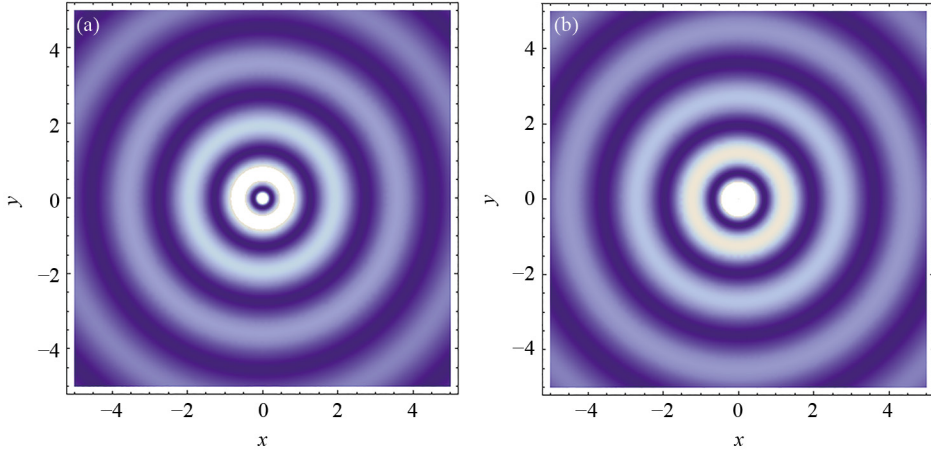


Figure 3. Optical ring structures in the intensity profiles of the components (a) A_x and (b) A_y of laser vortex with parameters $m = 4$ and $\alpha = 4$

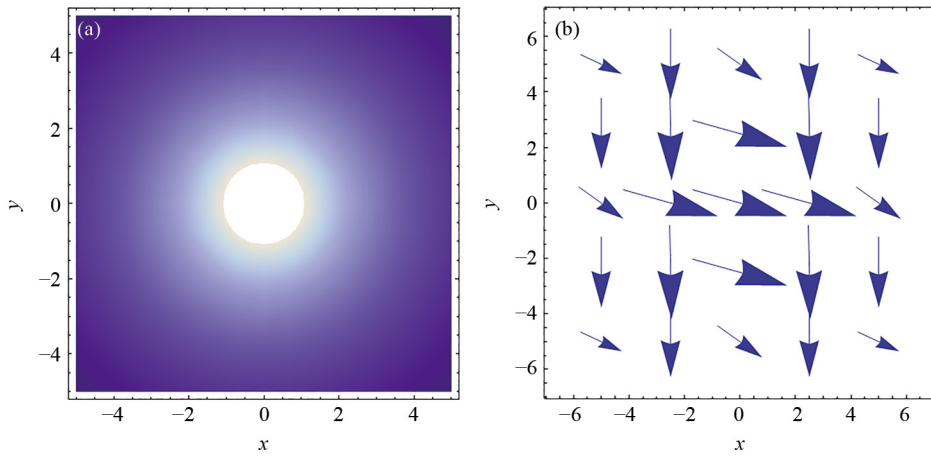


Figure 4. Graph of (a) the total intensity profile and (b) vector diagram of optical vortex with parameters $m = 4$ and $\alpha = 4$

In intensity profiles in Figure 2 and Figure 4, the absence of ring structures is clearly seen. As already mentioned before this is a result of the compensation of minima in A_x with the maxima in A_y components and vice versa. The presence of amplitude-type vortices is registered by the vector diagram, visualizing the depolarization of the electric field of the pulses. The spot of the pulse does not change with the increase of the value of the vortex parameter m . The vector diagrams show different patterns in the orientation of the vector electric field of vortices for $m = 2$, $m = 4$, and $\alpha = 4$.

4. Conclusion

The study of optical vortices in fibers with a step-index profile and anomalous dispersion, taking into account the influences of the third-order dispersion and the dispersion of nonlinearity, contributes to the improvement of the current methods for transfer of information and offers new implementations in a number of other technological fields. We have demonstrated that the evolution of such type of light pulses is described by a system of two nonlinear partial differential equations for the A_x and A_y components of the vector amplitude function. This system was analytically studied and as a result, we found new classes of exact solutions. They characterize the features in the dynamics of ultra-short laser vortices in optical fibers with a step-index profile under these higher-order dispersive and nonlinear phenomena. The obtained

structures have amplitude-type singularity and they strongly depend on the vortex parameter m , which determines the number of ring structures in the optical vortices. Nonlinear parameters γ and s are involved in the expression for the vortex parameter m . The second and third-order dispersion changes the phase of the optical pulse components. It turns out that β does not directly affect the formation of the optical vortex.

Figures of the exact analytical solutions done for two different values of the vortex parameter m and parameter $\alpha = 4$ are presented. Vortices are in the form of concentric circles. They are observed only in the intensity profiles of the A_x and A_y components of the vector amplitude function \vec{A} . The width of the rings in the components varies depending on the values of the vortex parameter and the number of oscillations under the pulse envelope. When the value of the vortex parameter m grows, the number of rings in the intensity profile of the corresponding component of the laser pulse increases as well and the width of the rings decreases. The vector diagram demonstrates the depolarization in the spot of the laser pulse. It is observed that the orientation of the vector electric field in the total intensity profile of the vortex changes for different values of the parameter m . These results are important for the development of modern photonic technologies.

The amplitude vortices are significantly influenced by the medium in which the optical pulse propagates. This plays an important role in the formation of the optical structure, as we assume that for different complex profiles of the refractive index of the medium, different vortex structures will form. This opens new perspectives for investigations in the field of optical vortices and their dynamics in different waveguides.

Acknowledgement

The present article is supported by Bulgarian Ministry of Education and Sciences by grant DO1-184/01.08.2022.

Conflict of interest

The authors declare no competing financial interest.

References

- [1] Li Z, Zhang M, Liang G, Li X, Chen X, Cheng C. Generation of high-order optical vortices with asymmetrical pinhole plates under plane wave illumination. *Optics Express*. 2013; 21(13): 15755-15764.
- [2] Li K, Tang K, Lin D, Wang J, Li B, Liao W, et al. Direct generation of optical vortex beams with tunable topological charges up to 18th using an axicon. *Optics and Laser Technology*. 2021; 143: 107339. Available from: <https://doi.org/10.1016/j.optlastec.2021.107339>.
- [3] Aksenov VP, Venedikov VY, Sevryugin AA, Tursunov IM. Formation of optical vortices by the use of holograms with an asymmetric fringe profile. *Optics and Spectroscopy*. 2018; 124(2): 273-277.
- [4] Hansinger P, Maleshkov G, Garanovich IL, Skryabin DV, Neshev D, Dreischuh A, et al. White light generated by femtosecond optical vortex beams. *Journal of the Optical Society of America B*. 2016; 33(4): 681-690.
- [5] Wang X, Nie Z, Liang Y, Wang J, Li T, Jia B. Recent advances on optical vortex generation. *Nanophotonics*. 2018; 7(9): 1533-1556.
- [6] Brunet T, Thomas J-L, Marchiano R. Transverse shift of helical beams and subdiffraction imaging. *Physical Review Letters*. 2010; 105: 034301. Available from: <https://doi.org/10.1103/PhysRevLett.105.034301>.
- [7] Coullet P, Gil L, Rocca F. Optical vortices. *Optics Communications*. 1989; 73(5): 403-408.
- [8] Heckenberg NR, McDuff R, Smith CP, Rubinsztein-Dunlop H, Wegener MJ. Laser beams with phase singularities. *Optical and Quantum Electronics*. 1992; 24: S951-S962. Available from: <https://doi.org/10.1007/BF01588597>.
- [9] Fatkhiev DM, Butt MA, Grakhova EP, Kutluyarov RV, Stepanov IV, Kazanskiy NL, et al. Recent advances in generation and detection of orbital angular momentum optical beams-a review. *Sensors*. 2021; 21(15): 4988.
- [10] Zhang K, Wang Y, Yuan Y, Burokur SN. A Review of orbital angular momentum vortex beams generation: From traditional methods to metasurfaces. *Applied Sciences*. 2020; 10(3): 1015.

[11] Porfirev AP, Kuchmizhak AA, Gurbatov SO, Juodkazis S, Khonina SN, Kulchin YN. Phase singularities and optical vortices in photonics. *Physics-Uspekhi*. 2022; 65(8): 789-811.

[12] Uren R, Beecher S, Smith CR, Clarkson WA. Method for generating high purity laguerre-gaussian vortex modes. *IEEE Journal of Quantum Electronics*. 2019; 55(5): 1-9.

[13] Maguid E, Chriki R, Yannai M, Kleiner V, Hasman E, Friesem AA, et al. *ACS Photonics*. 2018; 5(5): 1817-1821.

[14] Sroor H, Huang Y-W, Sephton B, Naidoo D, Vallés A, Ginis V, et al. High-purity orbital angular momentum states from a visible metasurface laser. *Nature Photonics*. 2020; 14(8): 498-503.

[15] Rui G, Wang X, Cui Y. Manipulation of metallic nanoparticle with evanescent vortex Bessel beam. *Optics Express*. 2015; 23(20): 25707-25716.

[16] Datta A, Saha A. Realization of a highly sensitive multimode interference effect-based fiber-optic temperature sensor by radiating with a vortex beam. *Optik*. 2020; 218: 165006. Available from: <https://doi.org/10.1016/j.ijleo.2020.165006>.

[17] Gahagan KT, Swartzlander GA. Optical vortex trapping of particles. *Optics Letters*. 1996; 21(11): 827-829.

[18] Khonina SN, Striletz AS, Kovalev AA, Kotlyar VV. Propagation of laser vortex beams in a parabolic optical fiber. In: *Proceedings of SPIE-The International Society for Optical Engineering*. USA: SPIE; 2009.

[19] Bolshtyansky MA, Savchenko AY, Zel'dovich BY. Use of skew rays in multimode fibers to generate speckle field with nonzero vorticity. *Optics Letters*. 1999; 24(7): 433-435.

[20] Kotlyar VV, Soifer VA, Khonina SN. Rotation of multimodal Gauss-Laguerre light beams in free space and in a fiber. *Optics and Lasers in Engineering*. 1998; 29(4-5): 343-350.

[21] Karpeev SV, Khonina SN. Experimental excitation and detection of angular harmonics in a step-index optical fiber. *Optical Memory and Neural Networks*. 2007; 16(4): 295-300.

[22] Ng J, Lin Z, Chan CT. Theory of optical trapping by an optical vortex beam. *Physical Review Letters*. 2010; 104(10): 103601.

[23] Wang X, Nie Z, Liang Y, Wang J, Li T, Jia B. Recent advances on optical vortex generation. *Nanophotonics*. 2018; 7(9): 1533-1556.

[24] Slavchev V, Dakova A, Gocheva N, Bozhikoliev I, Kovachev K, Biswas A. Laser ring structures in step-index fibers. *Journal of Physics: Conference Series*. 2022; 2339(1): 012007.

[25] Agrawal GP. *Nonlinear Fiber Optics*. 4th ed. New York: Academic Press; 2007.

[26] Han SH, Park QH. Effect of self-steepening on optical solitons in a continuous wave background. *Physical Review E*. 2011; 83(6 Pt 2): 066601.

[27] Yang H, Xiao G, Zhao S, Tang Z, Li T, Luo Y, et al. Impact of the self-steepening effect on soliton spectral tunneling in PCF with three zero dispersion wavelengths. *Chinese Optics Letters*. 2018; 16(7): 070601.

[28] De Oliveira JR, De Moura MA, Hickmann JM, Gomes ASL. Self-steepening of optical pulses in dispersive media. *Journal of the Optical Society of America B*. 1992; 9(11): 2025-2027.

[29] Yang H, Wang B, Chen N, Tong X, Zhao S. The impact of self-steepening effect on soliton trapping in photonic crystal fibers. *Optics Communications*. 2016; 359: 20-25. Available from: <https://doi.org/10.1016/j.optcom.2015.09.013>.

[30] Ahmed KK, Badra NM, Ahmed, HM, Rabie WB. Soliton solutions of generalized Kundu-Eckhaus equation with an extra-dispersion via improved modified extended tanh-function technique. *Optical Quantum Electronics*. 2023; 55: 299. Available from: <https://doi.org/10.1007/s11082-023-04599-x>.

[31] Seadawy AR, Ahmed HM, Rabie WB, Biswas A. An alternate pathway to solitons in magneto-optic waveguides with triple-power law nonlinearity. *Optik*. 2021; 231(1): 166480.

[32] Samir I, Ahmed HM, Mirzazadeh M, Triki H. Derivation new solitons and other solutions for higher order Sasa-Satsuma equation by using the improved modified extended tanh scheme. *Optik*. 2023; 274(2): 170592.

[33] Rabie WB, Ahmed HM. Construction cubic-quartic solitons in optical metamaterials for the perturbed twin-core couplers with Kudryashov's sextic power law using extended *F*-expansion method. *Chaos, Solitons and Fractals*. 2022; 160(1): 112289.

[34] El-shamy O, El-barkoki R, Ahmed HM, Abbas W, Samir I. Exploration of new solitons in optical medium with higher-order dispersive and nonlinear effects via improved modified extended tanh function method. *Alexandria Engineering Journal*. 2023; 68(6): 611-618.

[35] Alhojilan Y, Ahmed HM. Novel analytical solutions of stochastic Ginzburg-Landau equation driven by Wiener process via the improved modified extended tanh function method. *Alexandria Engineering Journal*. 2023; 72: 269-274. Available from: <https://doi.org/10.1016/j.aej.2023.04.005>.

- [36] Boyd RW. *Nonlinear Optics*. 3rd ed. Orlando: Elsevier Academic Press; 2008.
- [37] Dakova A, Murad Y, Kasapeteva Z, Dakova D, Slavchev V, Kovachev L, et al. Cnoidal waves and dark solitons with linear third-order dispersion and self-steepening effect. *Optik*. 2022; 270(80): 170035.
- [38] Kasapeteva Z, Dakova A, Krasteva S, Slavchev V, Dakova D, Kovachev L, et al. Bright solitons under the influence of third-order dispersion and self-steepening effect. *Optical and Quantum Electronics*. 2022; 54(6): 352.
- [39] Dakova-Mollova A, Miteva P, Dakova D, Slavchev V, Kasapeteva Z, Pavkov T, et al. Broad-band optical solitons. *Optik*. 2023; 279(10): 170770.